Available online at www.sciencedirect.com
SCIENCE DIRECT®
Journal of volcanology and geothermal research
ELSEVIER
Journal of Volcanology and Geothermal Research 124 (2003) 255–279
www.elsevier.com/locate/jvolgeores

Chaotic advection, fractals and diffusion during mixing of magmas: evidence from lava flows

D. Perugini [a,*], G. Poli [a], R. Mazzuoli [b]

[a] *Department of Earth Sciences, University of Perugia, Piazza Università 1, 06100 Perugia, Italy*
[b] *Department of Earth Sciences, University of Pisa, Via Santa Maria 53, 56126 Pisa, Italy*

Received 4 July 2002; accepted 3 March 2003

Abstract

Structures of magma mixing from three different lava flows have been analyzed and the degree of mingling has been quantified by measuring the contact perimeter between magmas and the fractal dimension of structures. In each lava flow, the values of these parameters suggest that the magma mixing structures were produced by chaotic dynamics induced by stretching and folding processes between the interacting magmas. The mingling of magmas has been simulated using a chaotic dynamical system consisting of repeated stretching and folding processes. The simulation shows the same patterns of variation of contact perimeter and fractal dimension as those observed in natural structures and indicates that magma interaction processes acted with different intensities in the three lava flows in response to different magmatic interaction regimes. Since physical dispersion of one magma inside another through stretching and folding processes and chemical exchanges are closely related, we performed coupled numerical simulations of chaotic advection and chemical diffusion. The results show a good agreement between the computed and natural structures, in particular, the occurrence in the same system of well- and poorly mixed regions. It is shown that magma interaction processes are able to generate magmatic masses having wide spatial heterogenity at many length scales. This occurrence can account for the presence of magmatic enclaves inside host rocks showing a variable degree of hybridization in both plutonic and volcanic environments.

Keywords: magma mixing; chaotic advection; fractals; chemical diffusion

1. Introduction

Magmatic interaction processes have been widely recognized and studied in plutonic and volcanic environments (e.g. Poli et al., 1996; Thomas and Tait, 1997; Blake and Fink, 2000). Although a considerable number of studies based on geochemical investigations, as well as on analog and numerical fluid dynamic simulations, have been reported (e.g. Oldenburg et al., 1989; Poli and Tommasini, 1991; Williams and Tobisch, 1994; Snyder and Tait, 1996; Weinberg and Leitch, 1998), only recently has it been suggested that the mixing of magmas can be studied using the principles of chaotic dynamics and fractal geometry (Flinders and Clemens, 1996; Ferrachat and

* Corresponding author. Tel.: +39-075-585-2652; Fax: +39-075-585-2603.
E-mail address: diegop@unipg.it (D. Perugini).

0377-0273/03/$ – see front matter © 2003 Elsevier Science B.V. All rights reserved.
doi:10.1016/S0377-0273(03)00098-2

Ricard, 1998; Perugini and Poli, 2000; Perugini et al., 2002; Poli and Perugini, 2002).

In this paper we analyze the structures produced by magma interaction in lava flows outcropping on the islands of Lesbos (Greece), Salina and Vulcano (Italy) using the concepts and methods of fractal geometry and chaos theory to quantify and model chaotic advection during the mingling of magmas. In particular the numerical simulation of magma mingling is carried out using a chaotic numerical system. In addition, since the mingling of magmas is closely associated with chemical diffusion, we coupled the model of chaotic advection with a chemical diffusion model in order to assess the ability of chaotic mixing to produce hybrid rocks bearing magmatic enclaves. We show how the onset of chaotic dynamics and the formation of fractal structures can account for rapid homogenization inducing chemical mixing of large volumes of magmas, a feature that cannot be explained by simple diffusion processes.

2. General features of magma mixing structures in lava flows

It has become accepted practice to apply the term 'magma mingling' to indicate the process acting to disperse physically (no chemical exchanges are involved) one or more magmas inside a host magma, whereas the term 'magma mixing' indicates that the mingling of magmas is also accompanied by chemical exchanges (e.g. Flinders and Clemens, 1996). In this paper we adopt the above conventions when it is possible to discriminate between the two processes.

It has been widely argued that magmas can mix efficiently only when their viscosities are similar (e.g. Sparks and Marshall, 1986; Grasset and Albarede, 1994; Bateman, 1995; Poli et al., 1996). Such physical conditions can occur when: (i) magmas have a similar viscosity from the beginning of the interaction process, and (ii) different magmas achieve a similar viscosity in response to evolutionary processes (e.g. Sparks and Marshall, 1986; Poli et al., 1996). Accordingly, we focus our attention on magmatic interaction processes when magmas have similar viscosities. In particular we study magma mixing structures in lava flows outcropping on the islands of Lesbos (Greece), Vulcano and Salina (Italy). These structures are studied because the mixed magmas (1) have been inferred to have similar density and viscosity (Table 1), and (2) provide instantaneous pictures of the ongoing magma mixing process thanks to eruption and rapid cooling.

The studied lava flows belong to volcanic islands having high-K and calc-alkaline affinity associated with subduction-related margins. Lesbos island belongs to a belt of subduction-related K-rich volcanism in North-Eastern Greece and Western Turkey (Pe-Piper, 1984; Pe-Piper and Piper, 1992). Salina and Vulcano belong to the Eolian magmatic arc: Salina is formed by calc-alkaline and HK magmatic products (e.g. Gertisser and Keller, 2000), whereas Vulcano is formed almost exclusively by HK and shoshonitic products (e.g. De Astis et al., 2000). In all the three islands, magma interaction has played an important role in the magmatic evolution (e.g. Pe-Piper and Piper, 1992; De Rosa et al., 1996; De Astis et al., 1997).

Several structures of magma interaction have been collected and studied from sections orthogonal to the main direction of motion of the lava flows (five for Salina, five for Vulcano, and five for Lesbos). These structures consist mainly of glassy rocks with less than 4% crystals (Fig. 1). Since the host magma in all three lava flows is always more acid than the 'dispersed' magma, we refer to the former as 'A' (acid) magma and to the 'dispersed' magma as 'B' (basic) magma (Table 1).

Macroscopic observations (Fig. 1) show that, in all three lava flows, magmas underwent mixing processes that produced an intimate dispersion of B magmas through A magmas. Moreover, inside the same system it is possible to observe the contemporaneous occurrence of (1) filament-like regions of B magmas inside A magmas (active regions, AR; Fig. 1), and (2) coherent regions of B magmas that are not dispersed through A magmas, showing a globular shape and occurring between filament-like regions (coherent regions, CR; Fig. 1; more details regarding these acronyms are given below). It is noteworthy that the

Table 1
Chemical analyses of A and B magmas in the lava flows of Salina, Vulcano and Lesbos performed on glasses by an electron probe micro-analyzer

	Salina		Vulcano		Lesbos	
	Magma A	Magma B	Magma A	Magma B	Magma A	Magma B
SiO_2	63.58	54.06	58.18	52.81	73.19	67.18
TiO_2	0.59	0.63	0.62	0.60	0.07	0.06
Al_2O_3	15.77	18.34	15.64	18.77	16.20	17.57
FeO_{tot}	6.40	8.77	7.87	8.90	0.97	1.34
MnO	0.10	0.19	0.74	0.68	0.14	0.11
MgO	1.99	4.60	1.81	2.48	0.65	1.90
CaO	4.04	8.98	5.32	8.94	1.01	2.01
Na_2O	4.68	2.74	4.92	3.78	3.57	3.03
K_2O	2.44	1.50	4.03	2.10	4.12	6.75
P_2O_5	0.41	0.21	0.89	0.83	0.39	0.21
Total	100.00	100.02	100.02	99.89	100.29	100.16
Rock	Latite	Andesite	Trachyte	Basalt	Rhyolite	Qz-Trachyte
μ (log Pas)	5.94	4.42	5.01	4.39	7.19	5.97
ρ (g/cc)	2.62	2.85	2.70	2.82	2.36	2.46

In the table are also reported viscosity (μ) and density (ρ) of the A and B magmas calculated from their geochemical compositions (Shaw, 1972) considering the following temperatures: Salina (A: 950°C; B: 1050°C); Vulcano (A: 1000°C; B: 1150°C); Lesbos (A: 900°C; B: 950°C) and anhydrous conditions.

occurrence of such structures during fluid mixing has been widely documented for both real and simulated systems (Fig. 2; e.g. Ottino et al., 1988; Liu et al., 1994a; Aref and El Naschie, 1995). Further observations show that filaments and globular portions of B magmas dispersed through A magmas are ubiquitous from the outcrop scale to the microscopic scale (Fig. 1C–F). This suggests that structures produced by magmatic interaction show scale invariance and hence can be regarded as natural fractals.

3. Quantitative analysis of magmatic interaction structures

3.1. Length of interfaces between magmas

In order to quantify the degree of mingling of the studied structures, grayscale pictures (Fig. 3A) have been processed using the NIH (National Institutes of Health) image analysis software to produce binary images in which the B and A magmas have been replaced by black and white colors, respectively (Fig. 3B). After thresholding, the length of interfaces (interfacial perimeter, IP) between A and B magmas was measured (Table 2) by counting the number of black pixels (B magma) in contact with white pixels (A magma). In all three lava flows the amount of B magma, measured on two-dimensional pictures, is quite constant and ranges from 48% to 51%. IP is a good estimate of the intensity of 'mingling' since it increases as the mingling process proceeds (e.g. Ottino et al., 1993; Liu et al., 1994a; Aref and El Naschie, 1995). To estimate the uncertainty on IP associated with the reduction of the original grayscale images to binary images, several measurements were performed on black and white images obtained using different threshold values. Results show that IP is estimated with an error better than 5%. Although IP shows different values within each lava flow, the structures of the Lesbos lava flow have, on average, higher IP values than Salina and Vulcano and, hence, they display a higher degree of mingling.

3.2. Fractal analysis

Since the studied structures show self-similarity and, hence, a fractal nature, we measured their fractal dimension using the box-counting tech-

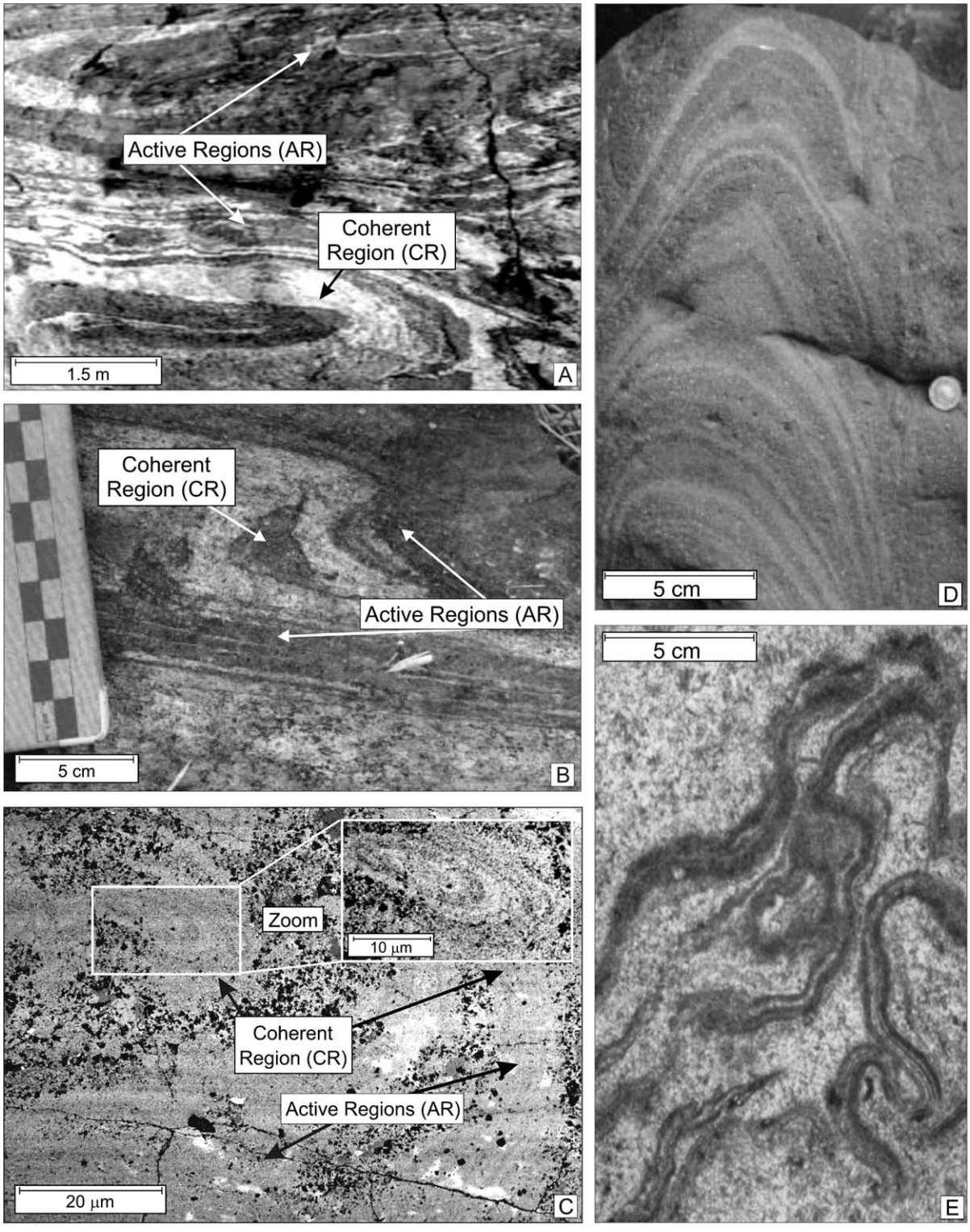
Active Regions (AR)
Coherent Region (CR)
1.5 m
A
Coherent Region (CR)
Active Regions (AR)
5 cm
B
Zoom
10 μm
Coherent Region (CR)
Active Regions (AR)
20 μm
C
5 cm
D
5 cm
E

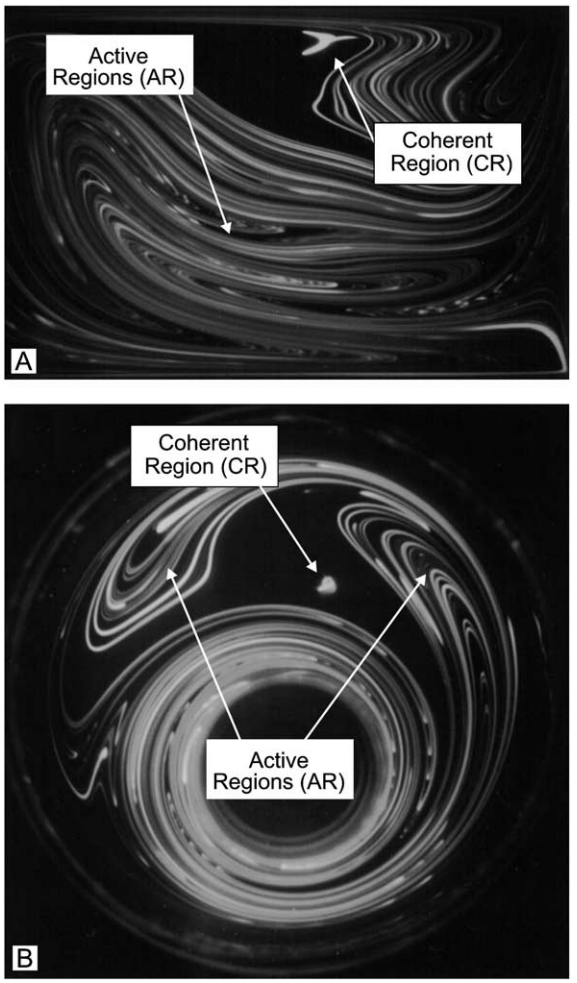

Fig. 2. Examples of chaotic fluid mixing experiments showing the same kind of structures observed in natural lava flows (from Bresler et al., 1997).

nique (D_{box}; e.g. Mandelbrot, 1982; Liebovitch and Toth, 1989). With this technique a square mesh of various size (r) is laid over the image and the number of boxes (N) that contain part of the image is counted (Fig. 3B). Mandelbrot (1982) shows that for fractal patterns the following relationship is satisfied:

$$N = r^{-D_{box}} \quad (1)$$

Using logarithms Eq. 1 can be also written as follows:

$$\mathrm{Log}(N) = -D_{box}\cdot\mathrm{Log}(r) \quad (2)$$

The fractal dimension (D_{box}) is calculated performing a linear interpolation of the Log(r) vs. Log(N) graph, and the slope of the linear interpolation is equal to $-D_{box}$ (Fig. 3C).

The fractal dimension calculated with this technique quantifies the degree of dispersion of one fluid inside another because D_{box} increases as the degree of mingling increases (e.g. Sreenivasan et al., 1989; Vorobieff et al., 1999); D_{box} is, thus, a robust and particularly suitable descriptor for quantifying the degree of mingling.

Fractal analysis has been performed on the same thresholded images used to calculate the IP (Fig. 3B,C) and D_{box} values are reported in Table 2. To estimate the uncertainty on D_{box} associated with the reduction of the original gray-scale images to black and white images, several measurements of the fractal dimension were performed on binary images obtained using different threshold values. The results show that D_{box} can be estimated with an error better than 0.005%. Similar results have also been reported by Sreenivasan et al. (1989) for analogous measurements.

The graph of Fig. 4 shows the variation of D_{box} against Log(IP) for the structures of the three lava flows. The use of Log(IP) is a convenient choice to appreciate better the relationships between these two parameters since IP values are more than one order of magnitude higher than D_{box} values. The patterns exhibited by the variation of the fractal dimension (D_{box}) against Log(IP) are linear for all three lava flows and the three linear trends have different slopes. In particular, structures from Lesbos define a trend having the highest slope with respect to Vulcano and Salina. These results show that Lesbos structures have

Fig. 1. Examples of magma mixing structures in lava flows from the island of Lesbos (A–C), Vulcano (D) and Salina (E). The dark flow structures consist of B magmas dispersed through light colored A magmas. In all lava flows mixing structures have the same patterns at many scales of magnification. Acronyms given to the different portions of the structures are related to their kinematic significance as explained later on in the text.

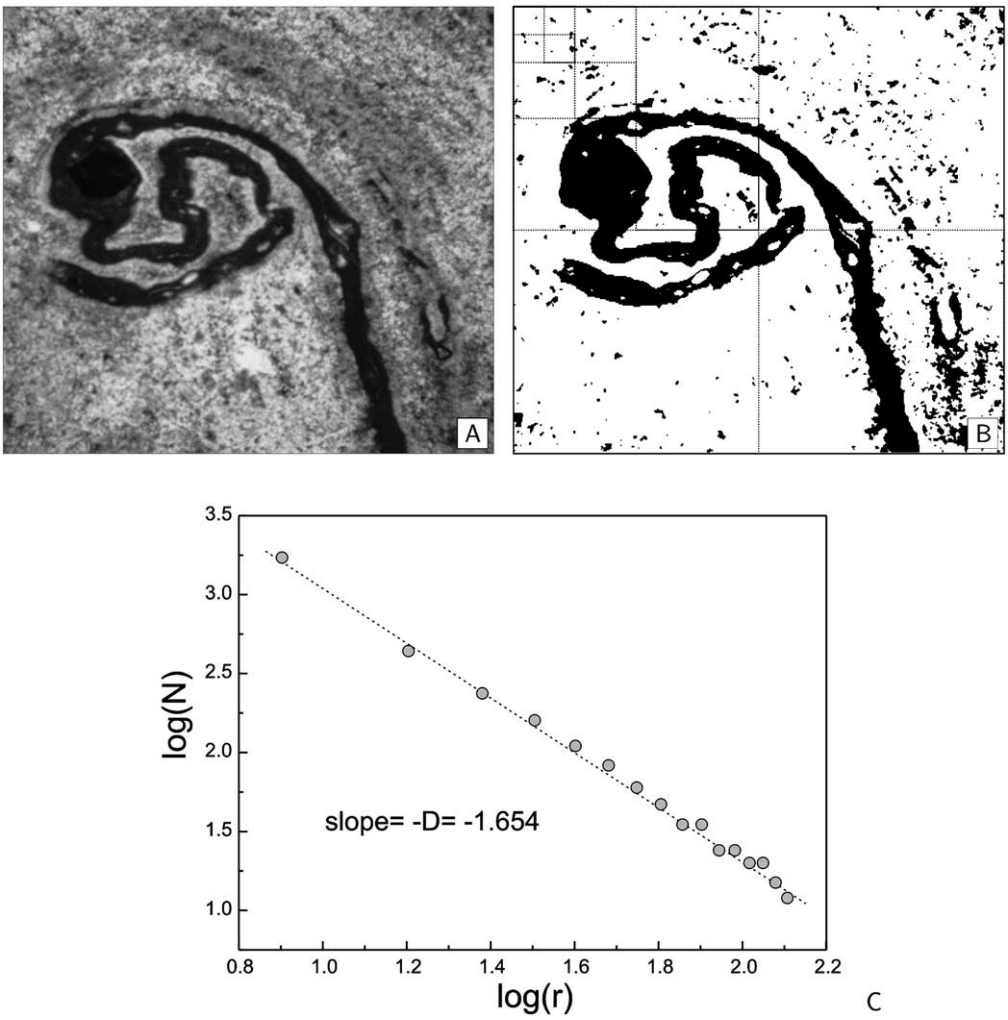

Fig. 3. (A) Example of a magma mixing structure; (B) thresholded structure on which IP and D_{box} have been calculated. For clarity, the box-counting procedure is shown only on one quadrant; (C) Log(r) vs. Log(N) plot used to estimate the fractal dimension (D_{box}) of magma interaction structures.

fractal dimensions higher than Vulcano and Salina at the same IP. Taking into account that higher D_{box} corresponds to higher degrees of mingling, the Lesbos lava flow underwent more vigorous mingling processes that produced more intimate dispersion of B magmas through A magmas than Vulcano and Salina lava flows.

3.3. Analysis of chemical exchanges between magmas

The above analysis provided information about physical dispersion (mingling) of magmas. However, physical dispersion and chemical processes cannot be thought to act independently because the higher is the physical dispersion, the greater the chemical exchanges by diffusion processes.

To assess whether chemical diffusion had occurred in the natural structures, electron microprobe analysis has been performed on traverses crossing filaments and a coherent region from one sample of the lava flow of Lesbos (AR and CR; Fig. 5A,D). Fig. 5B,C shows that the variations of K_2O and Al_2O_3 across the filaments dis-

play several continuous bell-shaped trends passing from one filament to another. A similar variation of K_2O and Al_2O_3 is exhibited by the data presented in Fig. 5E,F for the coherent region, with the difference that a plateau of constant values of K_2O and Al_2O_3 exists in the center of the coherent region. The higher and lower values of K_2O and Al_2O_3 shown in Fig. 5 can be considered as the values of the end members involved in the mixing process. Bell-shaped patterns are typical of chemical diffusion processes (e.g. Crank, 1975; Kuo et al., 1997), and this suggests that, even if the diffusion process was not very efficient in the lava flow of Lesbos because of the quenching of lavas, chemical diffusion acted between magmas.

4. Simulation of magma mingling

It has been widely documented in both fluid dynamic and numerical simulations that fractal structures generated by fluid mixing are closely associated with chaotic dynamics (e.g. Ottino et al., 1988; Liu et al., 1994a; Aref and El Naschie, 1995; Appendix A). In particular, the chaotic nature of fluid mixing systems and the occurrence of fractal domains are due to the action of stretching and folding processes between the interacting fluids (e.g. Ottino, 1989; Muzzio et al., 1992; Liu et al., 1994a; Aref and El Naschie, 1995). Stretching and folding are non-linearly coupled processes. The first induces elongation of fluids whereas the latter bends and redistributes them through the mixing system. The folding can be thought of as a consequence of stretching. Thus, fluids cannot be stretched ad infinitum because of the finite size of the geometrical framework in which the mixing process occurs, and, as a consequence, fluids must fold over themselves. This kind of kinematical evolution of the mixing system generates lamellar structures with a wide distribution of length scales that span many orders of magnitude and define fractal domains (e.g. Alvarez et al., 1998; Ottino et al., 1993; Appendix A).

Table 2
Values of fractal dimension (D_{box}) and IP of the analyzed magma mixing structures

	Lesbos	Salina	Vulcano
Interfacial perimeter IP (in cm)			
Structure n. 1	112	45	85
Structure n. 2	156	86	101
Structure n. 3	290	136	178
Structure n. 4	338	213	252
Structure n. 5	582	358	460
Fractal dimension (D_{box})			
Structure n. 1	1.736	1.674	1.691
Structure n. 2	1.784	1.704	1.721
Structure n. 3	1.857	1.727	1.761
Structure n. 4	1.880	1.755	1.786
Structure n. 5	1.927	1.787	1.824

IP has been measured counting the number of contact pixels between A and B magmas, and rescaling to centimeters.

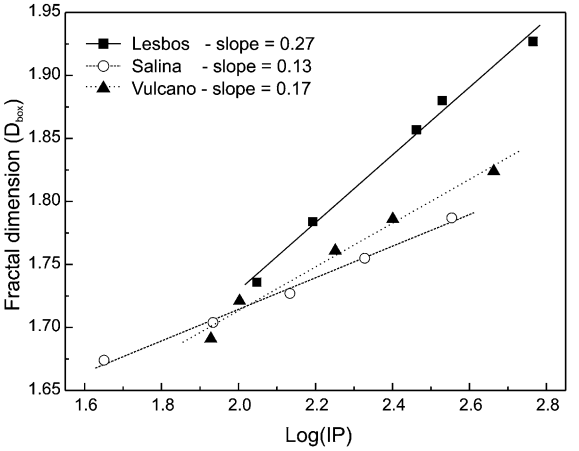

Fig. 4. Variation of fractal dimension (D_{box}) vs. Log(IP) for natural structures belonging to the three studied lava flows. In the graph are also reported the values of the slopes calculated by linear regression.

The studied magma mixing structures display morphological structures that can be recognized at many length scales (Fig. 1) and they have been demonstrated to be fractals (Fig. 3). Moreover, the filament-like structures and coherent regions, found in the analyzed lava flows, are also found in fluid mixing systems governed by chaotic dynamics (Fig. 2; e.g. Ottino et al., 1988; Liu et al., 1994a; Aref and El Naschie, 1995; Appendix A). These considerations favor the hypothesis that the structures observed in the three lava flows may be the product of chaotic dynamics.

Several physical processes can induce stretching and folding dynamics inside magmatic interaction

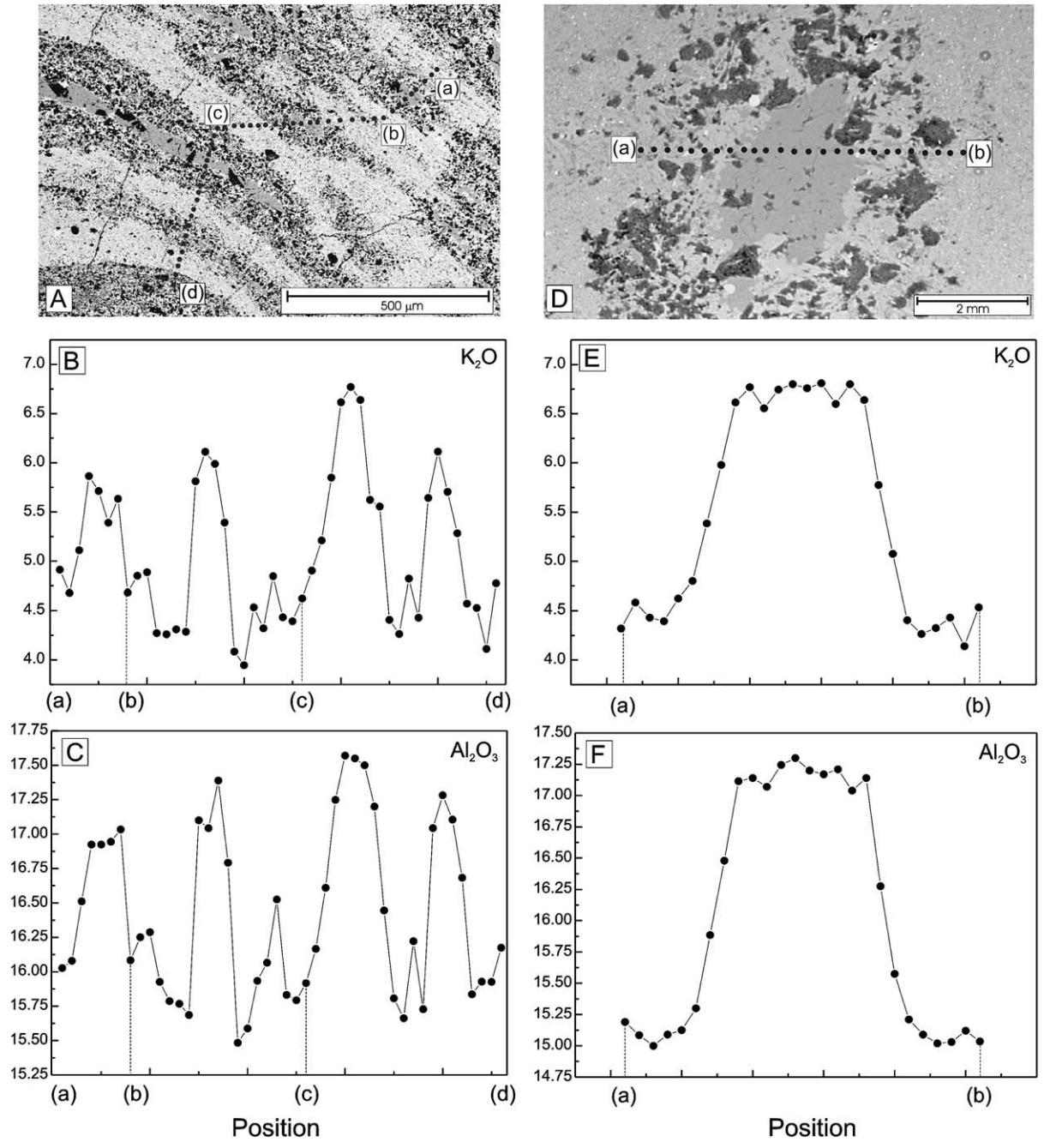

Fig. 5. Back scattered electron images of filament-like structures (A) and a coherent region (D) of the B magma inside the A magma from one sample of Lesbos lava flow. The pictures also show the location of the analyzed points. Variation of K_2O and Al_2O_3 across the filament-like structures (B and C) and the coherent region (E and F). Potassium and aluminum have been chosen because these elements have very different diffusion coefficients and for this reason they are particularly suitable for monitoring chemical diffusion (e.g. Baker, 1990; Schreiber et al., 1999). Other elements show similar patterns. Precision for K_2O and Al_2O_3 is estimated to be better than 4% and 3%, respectively.

systems. The most important processes acting to promote the dispersion of one magma inside another are: convection movements and plume-like dynamics of a light magma inside a denser one (e.g. Bateman, 1995; Cruden et al., 1995; Snyder and Tait, 1996; Cardoso and Woods, 1999), forced and fountain-like intrusions (e.g. Campbell and Turner, 1986), flows in conduits from different crustal levels up to eruption (e.g. Koyaguchi, 1985; Blake and Campbell, 1986; Koyaguchi and Blake, 1989). Most of these processes have been extensively studied using both experiment and numerical simulations, and it has been evidenced that such processes are strictly related to the onset of stretching and folding dynamics between fluids (e.g. Metcalfe et al., 1995; Hydon, 1995; Meleshko and Van Heijst, 1995). The investigation of the specific dynamics that produced the structures in the studied lava flows is beyond the scope of this paper. However, it is noteworthy that although all the above processes may have had a role in the genesis of those structures, there is evidence, especially for the Salina lava flow, that suggests a major role was played by flows in conduits and in sub-aerial channels (De Rosa et al., 1996; Perugini et al., 1999).

4.1. Iterated maps as kinematical template to simulate mingling of magmas

In order to simulate the process of dispersion of one magma inside another a chaotic dynamical system consisting of repeated stretching and folding processes has been used. The model belongs to a class of systems represented by a set of two coupled non-linear equations known as iterated maps (e.g. Ottino et al., 1988; Collet and Eckman, 1980; Sepulveda et al., 1989; Appendix A). It has been shown by several authors that this kind of system is suitable for understanding the dispersion of one fluid inside another, since it reproduces the morphological structures observed in real mixing systems independently from the geometries in which the process occurs (e.g. Liu et al., 1994a; Ott and Antonsen, 1989). This aspect is particularly important when the study is focused on structures produced by fluid mingling for which the exact geometry is unknown. This is the case for the structures studied in this paper because it is possible to observe only instantaneous pictures of the process. It is also important to note that iterated maps are suitable for simulating mingling processes between fluids having a similar viscosity (i.e. one fluid acts as a passive tracer; Appendix A). As it has been discussed previously, in all the three studied lava flows magmas have a similar viscosity (Table 1) and, thus, the assumption that a magma acts as a passive tracer is satisfied. Therefore, in our case iterated maps can be used as kinematical models to study the topology of flow fields during mingling of magmas.

The iterated map that we consider is known as the 'sine flow' map (hereafter map; e.g. Liu et al., 1994a; Clifford et al., 1998, 1999). The flow is defined by two motions:

$$x_{n+1} = x_n + \frac{k}{2}\cdot\sin(2\pi\cdot y_n) \quad [\mathrm{mod}1]$$
$$y_{n+1} = y_n + \frac{K}{2}\cdot\sin(2\pi\cdot x_n) \quad [\mathrm{mod}1] \tag{3}$$

It forms a two-dimensional conservative (area preserving) chaotic system whose domain is $0 \leq (x,\ y) \leq 1$ and where k is the parameter of the map. From a kinematical point of view, the flow is the combination of two orthogonal motions, each with a sinusoidal velocity profile. Many different velocity profiles can be utilized to reproduce chaotic systems (sinusoidal, exponential, power law; e.g. Aref and El Naschie, 1995). The 'sin-flow' map has been utilized in this paper because it is a well studied chaotic system (e.g. Liu et al., 1994a; Clifford et al., 1998, 1999), and it has been successfully utilized to simulate mixing of magmas (Perugini et al., 2003). However, it is to note that changing the velocity profile the structure of presented results does not change. The flow is defined on the two-dimensional torus meaning that whenever a particle exits the unit square, it re-enters the box through the opposite side. Since this model flow is continuous and everywhere differentiable in any order (including the boundaries), the imposition of periodic boundary conditions does not result in unphysical points (cusps) in the iteration of the map. As pointed out by other authors (e.g. Liu et al., 1994a; Clifford et al., 1998, 1999), this flow

scheme is useful for understanding chaotic mingling, because a variety of flow behaviors can be obtained by varying parameter k.

The flow field related to the map for different values of parameter k can be visualized by iterating a number of points belonging to the domain of the map for a large number of iterations. This operation produces the structures presented in

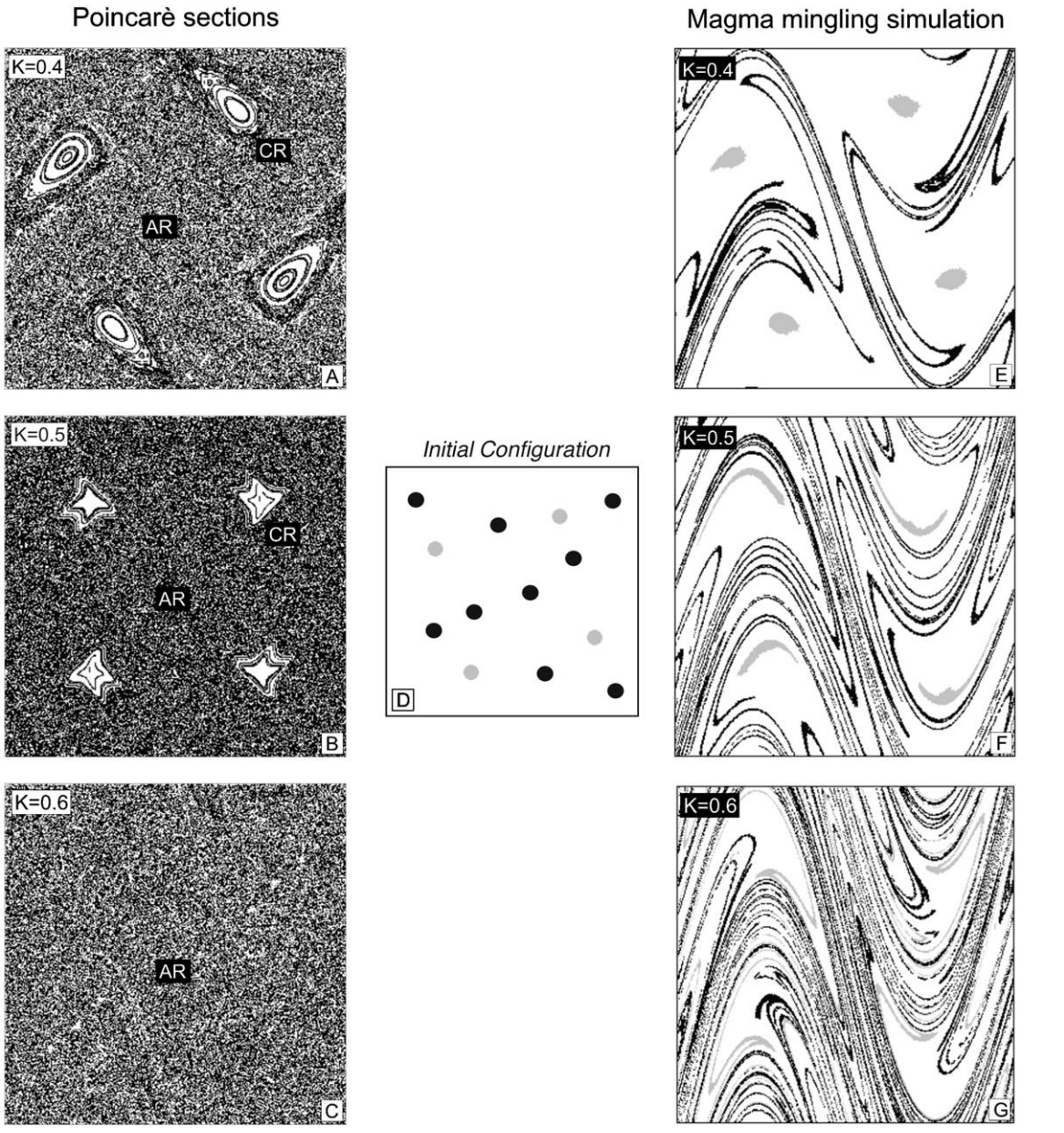

Fig. 6. Poincaré sections associated with the 'sine flow' map for different values of parameter k (A–C). Initial configuration of the magma mingling simulation (D): blobs of B magma are placed inside AR and CR, respectively; the blobs placed inside CR have been colored light gray. Mingling structures representing the state of the system after four iterations of the map for different values of k (E–G).

Fig. 6A–C that represent the Poincaré sections of the flow (e.g. Ottino et al., 1988; McCauley, 1993; Appendix A), and reflects the state to which the system converges, that is the system is attracted to these states, for different values of k. The images show that regular regions, consisting of closed trajectories, coexist with irregular regions, where precise trajectories cannot be defined and where the points are iterated in a more irregular way.

Bearing in mind that the efficiency of mingling lies in the ability of the components involved in the process to spread across the system, possibly in an irregular way (e.g. Ottino et al., 1988; Liu et al., 1994a), it follows that irregular and regular regions of the map are regions where fluids are well mingled (active regions, AR) and poorly mingled (coherent regions, CR), respectively.

Fig. 6A–C also provides insight into the effects of parameter k on the structures (AR and CR) produced by the map. In fact, CR are found to shrink as k increases (from Fig. 6A to C), and, at higher k values, they are reduced considerably in size leaving most of the space to AR. As shown by Bresler et al. (1997) the genesis of CR is closely related to the efficiency of stretching and folding dynamics and, in particular, CR form where stretching and folding dynamics are less efficient. k is hence a parameter regulating the efficiency of stretching and folding, and it is closely related to the degree and to the efficiency of the mingling process. The efficiency of the mixing process depends on many physical parameters such as viscosity, density, thermal and chemical gradients etc. The possibility to explore different mixing intensities varying a single parameter (k) makes iterated maps very useful prototypical systems to study the complexity inherent to mixing processes.

To follow the mingling process induced by the iteration of the map, we considered the initial configuration presented in Fig. 6D, in which blobs of a magma (colored circles) are placed inside another magma (white colored square). The choice of using initially circular blobs of B magma is motivated by the observation that the most poorly mingled magmas are characterized by blobs of mafic magma in a more felsic host (e.g. Blake and Fink, 2000; Bacon, 1986). This initial configuration fits well with field observations in which the mingling process has been 'frozen' at its initial stages. However, it is stressed that changing the initial shape of the B magma does not influence the structure of the results.

Light gray blobs were placed inside coherent regions (CR), whereas black blobs were placed inside the active regions (AR). The simulation was performed for different values of k. The outcome after four iterations is shown in Fig. 6E–G. Blobs inside AR mingled intimately due to the high stretching and folding rate they experienced, whereas blobs inside CR did not undergo vigorous stretching and folding processes but remained as discrete entities for low values of k. As k increases, CR reduce in size and are progressively replaced by AR, causing the light gray blobs to become progressively more dispersed.

The sine flow map can be used to compare the differences in the variation of contact perimeter in AR and CR as the number of iterations of the map increases (Fig. 7). The results indicate that blobs initially placed in the CR show weak fluctuations of the contact perimeter (Fig. 7) and this is mainly due to the fact that these blobs are only translated and rotated by the flow fields producing weak deformation of their initial shape iteration after iteration. On the other hand, a clear exponential increase of the contact perimeter against the number of iterations of the map is

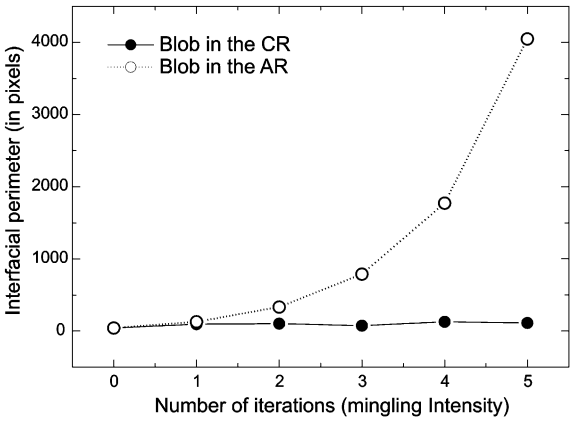

Fig. 7. Graph showing the variation of interfacial area of two blobs placed initially into an AR and a CR, respectively, during the iteration of the map considering a value of k equal to 0.4.

shown by the blobs initially placed in the AR, due to the high stretching and folding rate they experienced (Fig. 7). This clearly indicates that the overall contribution to an increase in the contact perimeter between the two magmas is given by the dispersion of blobs inside active mixing regions, whereas blobs inside coherent regions do not substantially contribute to an increase of the contact perimeter.

4.2. Comparison between simulated and natural magma mingling structures

There is a striking similarity between the structures obtained numerically (Fig. 6E–G), and the structures occurring in lava flows (Fig. 1). In particular the two types of kinematic structures represented by irregular and regular regions (AR and CR), where magmas are subjected to different degrees of mingling, can be recognized in nature and modeled systems (compare Figs. 1, 2 and 6E).

Starting from the initial configuration shown in Fig. 6D, we simulated the development of mingling structures using different values of parameter k for five iterations of the map. At every iteration we measured the IP and the fractal dimension (D_{box}), as for natural structures. The variation of D_{box} against Log(IP) is reported in Fig. 8. It shows that D_{box} increases linearly with Log(IP) as in the case of natural magmatic interaction structures (compare with Fig. 4). Furthermore, the linear trends have an increasing slope as k increases (Fig. 8). Since k regulates the efficiency of mingling inside the system, increasing slope values correspond to a higher mingling efficiency. It is worth noting that tests have been performed using different amounts of B magma considering the same values of k and results have shown that, although D_{box} and IP change in absolute values, slope values do not change. This evidences that slope values do not depend on the amount of B magma, but only on the dynamic regime responsible for mingling of magmas and, as such, they are robust descriptors to quantify the mingling efficiency that magma experienced. These results indicate that the three linear trends exhibited by the magma mixing structures belonging to the three different lava flows (Fig. 4) can be considered as three different magmatic systems, in which the stretching and folding processes dispersing the B magma inside the A magma acted with different intensities. In particular, it is suggested that mingling intensity increases from Salina to Lesbos.

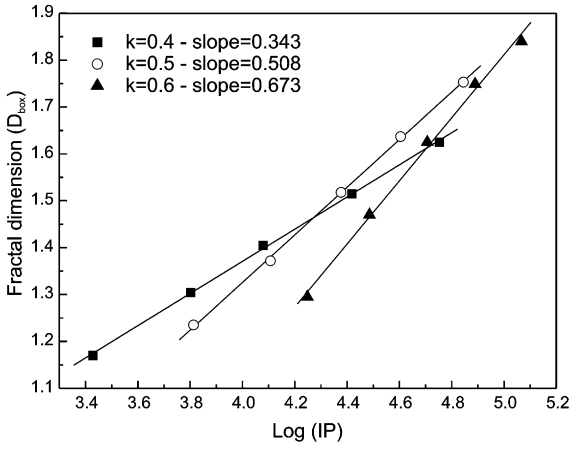

Fig. 8. Variation of fractal dimension (D_{box}) vs. Log(IP) for the magma mingling structures simulated using the map at different values of k. In the graph are also reported the values of the slopes calculated by linear regression.

5. Simulation of magma mixing

Fig. 5A,D shows an important difference in the spatial distribution of A and B magmas in the active and coherent regions, respectively: active regions are composed by alternate bandings of A and B magmas that are in contact through a large number of interfaces with respect to the coherent region of B magma, where the contact with the A magma is restricted to a single contact interface. Considering that chemical diffusion strongly depends on the extension of interfaces (e.g. Crank, 1975; Kuo et al., 1997), it is reasonable to suppose that the time required for homogenization is less for the filaments than for the coherent region. These considerations are corroborated by the variation of chemical elements through the filaments and the coherent region. Among filaments of Fig. 5A only one has the original concentration of K_2O and Al_2O_3 of the 'original' B magma (Table 1), whereas all the

other filaments have lower values. The filament having the highest K_2O and Al_2O_3 concentrations is the one having the greatest thickness, confirming that chemical diffusion is strongly dependent on the spatial distribution of magmas. Completely different is the case of K_2O and Al_2O_3 variation in the coherent region that, apart from the boundaries where diffusion becomes evident, shows constant values similar to those of the 'original' B magma in a wide portion of the CR (Fig. 5E,F). Thus, in the same system and in the same time span, the different regions show very different behaviors regarding the development of chemical diffusion processes.

The above considerations provide information on the potential rate of molecular diffusion during magmatic interaction. Chemical diffusion in magmas is a very slow process, since typical diffusion coefficients for chemical elements are in the order of 10^{-8}–10^{-10} cm^2/s (e.g. Baker, 1991; Chekhmir and Epel'baum, 1991). The temporal scale for chemical diffusion to occur efficiently is of great importance and needs to be addressed. Using the diffusion equation for objects with spherical and planar boundaries (Crank, 1975), it can be calculated that small portions of magmas, 1–3 cm in size, can be completely homogenized in times ranging from 10^2 to 10^5 years depending on the magnitude of the diffusion coefficients (see Baker, 1990 for details). Comparing these time scales to the possible lifetimes of magmas in magma chambers (ca. 3–360 ka; e.g. Volpe and Hammond, 1991; Davies et al., 1994; Heath et al., 1998), it becomes clear that chemical diffusion can have time to homogenize only small volumes of magma, orders of magnitude less than the typical volumes of magma chambers (10^{-1}–10^3 km^3; e.g. Woods and Pyle, 1997; Pietruszka and Garcia, 1999). As shown above, however, stretching and folding processes dramatically reduce the distances between the interacting magmas and produce fractal structures that propagate inside the magmatic masses from the metric to the micrometric scale (Figs. 1 and 6). This suggests that chemical diffusion can propagate quickly through large volumes of magmas because of the fractal nature of the structures produced by stretching and folding processes. In this dynamical context, where the entity of mixing (chemical exchanges) depends to such a large extent on the mingling rate (physical dispersion, stretching and folding), filament-like regions (AR) can be readily homogenized by chemical diffusion processes leading to conspicuous volumes of hybrid magmas. In contrast, in the same time span, coherent regions are not likely to be readily homogenized with the surrounding host because of their persistence as discrete islands.

5.1. Iterated maps and chemical diffusion to simulate mixing of magmas

To investigate the interplay between chaotic advection and chemical diffusion, we coupled the numerical model of chaotic advection of blobs of B magma inside A magma (using the sine flow map) with chemical diffusion processes using the algorithmic approach reported by Pierrehumbert (1995). We defined a continuous concentration field $c(x, y)$ on the plane, and spatially discretized it to a regular grid $c_{ij} = c(x_i, y_j)$. For the initial configuration (Fig. 9A), the black blobs (B magma) have a concentration equal to zero (corresponding to the black color in terms of coded colors), whereas the white host (A magma) has a concentration equal to 255 (corresponding to the white color in terms of coded colors). The map was first used to rearrange $c(x, y)$ through mapping (x, y) and re-interpolating to the grid. This iteration was followed by the diffusion step:

$$c_{ij} = (1-A)\cdot c_{ij} + \frac{1}{4}\cdot A\cdot[c_{(i+1)j} + c_{i(j+1)} + c_{(i-1)j} + c_{i(j-1)}] \quad (4)$$

where $0 < A < 1$ plays the role of the diffusion coefficient. This numerical scheme is a typical finite difference system (e.g. Crank, 1975) and corresponds to the discretization of the diffusion Laplace equation (e.g. Jain, 1989). c_{ij} is updated to new colors ranging from zero to 255 according to the diffusion that each cell underwent calculated using Eq. 4. After several iterations of the map coupled with the diffusion step, the concentration field $c(x, y)$ will have changed. Bearing in mind that the simulation was carried out using shades of gray, the concentration of each single

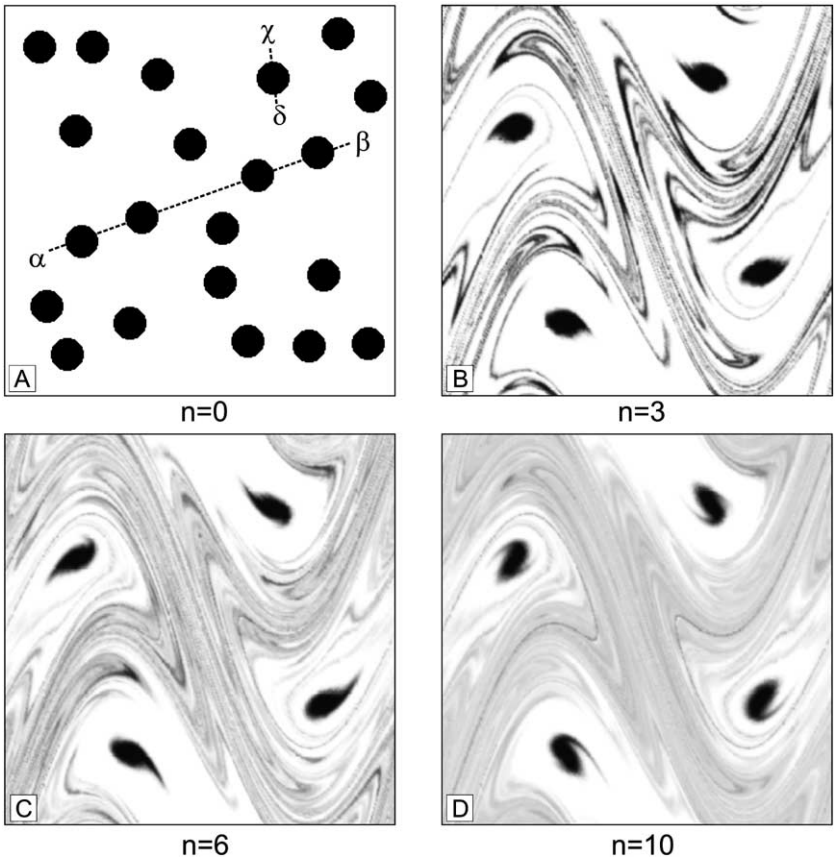

Fig. 9. Pictures showing the development of chemical diffusion processes simulated by the algorithms reported in the text for both CR and AR. Initial configuration (A); configurations of the system after a number of iterations of the map (n) equal to 3, 6, and 10, respectively (B, C, and D). Dashed lines in A represent traverses used to monitor the chemical diffusion process through AR and a CR as presented in Fig. 10.

cell will range from 0 to 255. Fig. 9 presents some of the steps of a simulation for k equal to 0.4. Since the focus here is on the relative differences in the rate of chemical diffusion between the active regions and the coherent regions and not about absolute values of chemical exchanges between magmas, A is kept constant to 0.5. Varying A will only reduce ($A > 0.5$) or increase ($A < 0.5$) the relative number of iterations of the simulation required to obtain the patterns of Fig. 9, and it does not influence the structure of reported results.

After 10 iterations of this simulation the filament-like structures have almost completely disappeared and have been replaced by a large and fairly homogenous region (Fig. 9D). On the other hand, after the same number of iterations (Fig. 9D), coherent blobs of the B magma are still easily recognizable, because the diffusion process did not homogenize them with the host magma. These results can also be readily observed in Fig. 10, which shows the variation of c_{ij} along two traverses passing through the filaments and through a blob (Fig. 9A).

As the number of iterations increases, the original identities of A and B magmas are progressively lost within filaments and this induces intermediate concentrations proportional to the initial masses of the two magmas. In contrast, at the same number of iterations, in large portions within the coherent region the original composition of magmas is maintained, although its concentration

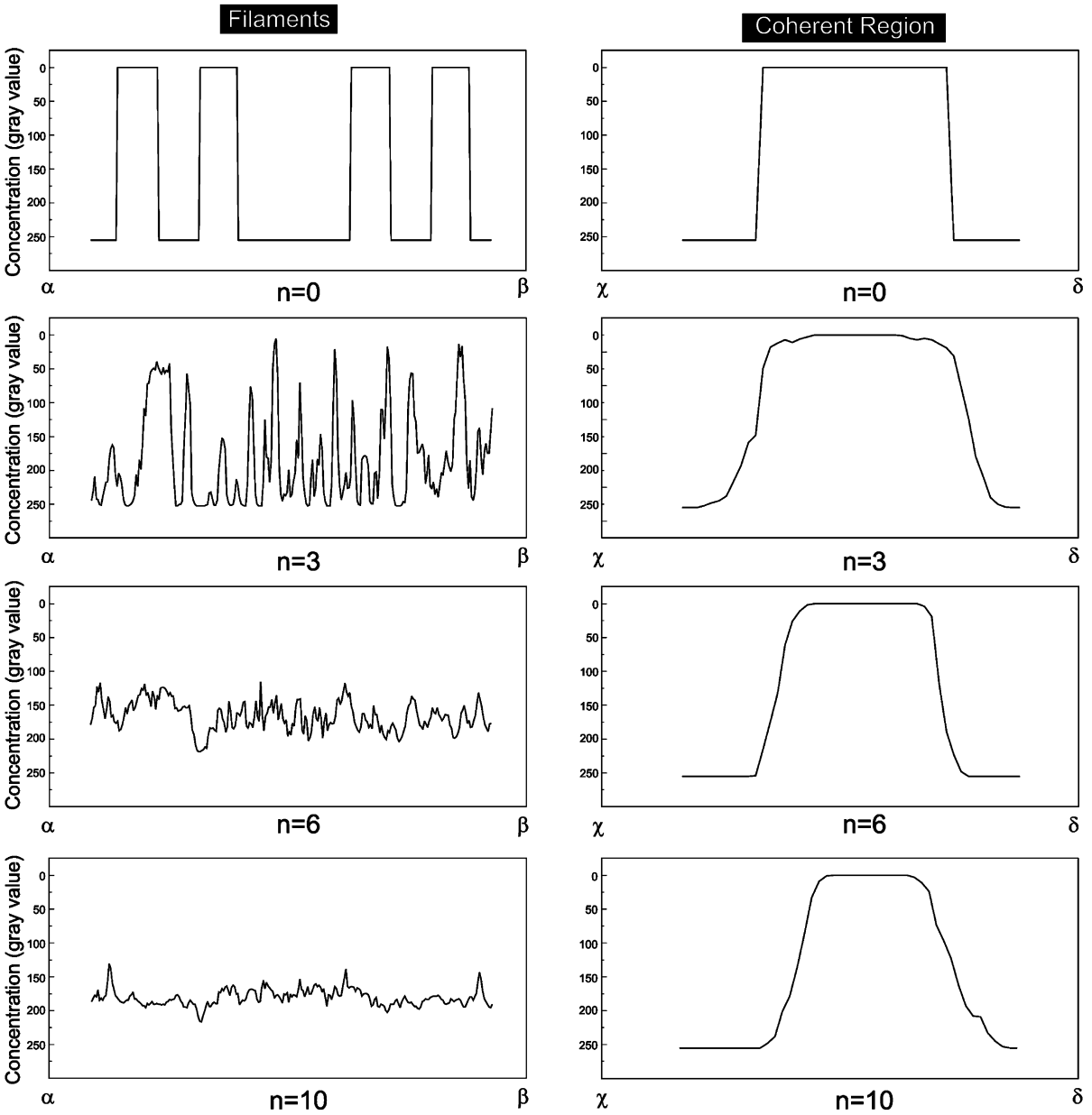

Fig. 10. Diagrams showing the distribution of gray values along the traverses presented in Fig. 9A at different numbers of iterations. Grayscale values are considered as proxy for concentration as reported in the text.

is slightly smoothed at its boundaries (Fig. 10). This result is directly related to the different dynamics that magmas suffer inside AR (high stretching and folding, increasing interfacial areas) and CR (low stretching and folding, constant interfacial area; Fig. 7).

5.2. Comparison between simulated and natural magma mixing structures

The modeled diffusion patterns of Fig. 10 closely resemble those found in natural systems (Fig. 5). Similarities are more evident in the dif-

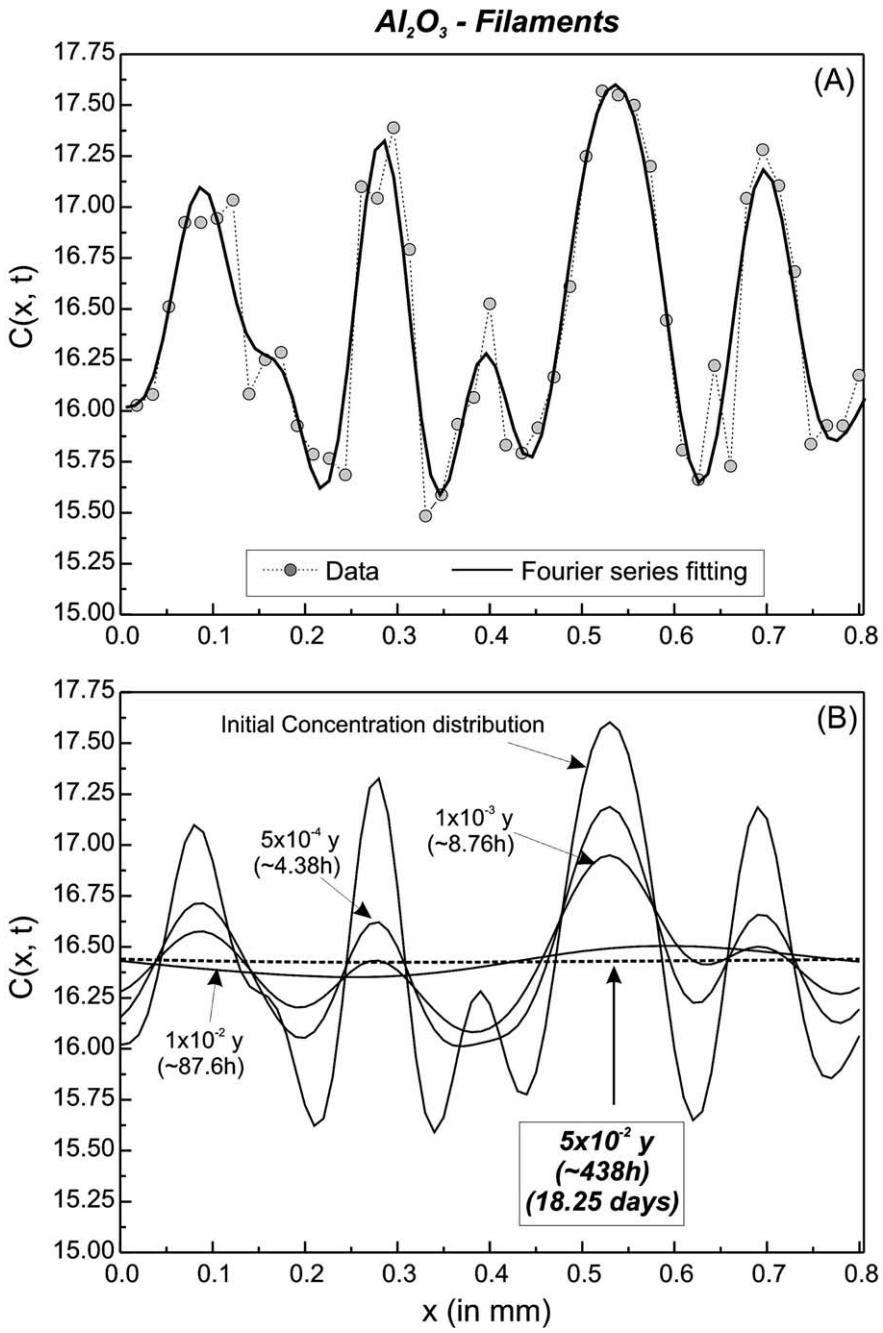

Fig. 11. Fourier series fitting (solid line) of the variation of Al_2O_3 through the filaments of Fig. 5A (A). Variation of $C(x, t)$ against x at different times for Al_2O_3 across filaments (B). The dashed line in B represents the reached homogenization of the system.

fusion patterns at low numbers of iterations (i.e. $n = 3$), where evidence of the original concentrations of the A and B magmas remained in both nature and simulation (compare Figs. 5 and 10). This is consistent with the fact that the rate of chemical diffusion in the natural structures has been inhibited by the rapid cooling of the magmatic masses that allowed the original compositions of A and B magmas to remain almost unaltered.

Although the above results give information on the relative differences in the rate of chemical diffusion between simulated AR and CR, it is worth discussing the time span in which chemical diffusion can act in natural AR and CR. This can be done starting from the AR and CR shown in Fig. 5A,D and calculating the time after which they would have been completely homogenized, assuming that magmas did not quench. The time of homogenization is calculated using the numerical solution of the diffusion equation for an infinite medium with an initial concentration $C_0(x, t)$ being a periodic function in space (Albarede, 1995; eq. 8.5.8, p. 434):

$$C(x, t) = C_0(x)\exp\left(-\frac{4\pi D t}{\lambda^2}\right) \quad (5)$$

where x is the space, t is the time, D is the diffusion coefficient and λ is the wavelength. The variation of concentration through the filaments and the coherent region is fitted using the Fourier series technique (Figs. 11A and 12A) whose polynomial expansion is used as the periodic function in the calculations of the diffusion patterns (Albarede, 1995).

Complete homogenization implies that at a certain time no more trace of the original structures exists in the system. This requires that the time for complete homogenization is estimated for chemical elements having the lowest diffusion coefficients. Among them Al_2O_3 has a very low diffusion coefficient (1×10^{-10} cm^2/s; Baker, 1990) in magmas similar to those constituting the mixing structures of Lesbos. Thus, the calculation of the homogenization time is performed considering Al_2O_3.

Figs. 11A and 12A show the fitting of Al_2O_3 data of Fig. 5C,F by Fourier series expansion along with the measured values. Figs. 11B and 12B show the variation of concentration $C(x, t)$ against distance (x) with the passing of time for the filaments and the coherent region, respectively. The concentration variation $C(x, t)$ continues to define patterns analogous to those observed in the natural (Fig. 5) and the simulated magma mixing structures (Fig. 10) that are, however, progressively smoothed with time in both AR and CR. The results indicate that the time required for the complete homogenization of filaments is more than two orders of magnitude lower than the time required for complete homogenization of the coherent region: filaments are homogenized in about 18 days whereas the time of homogenization for the coherent region is about 10 years.

6. Summary and conclusions

The study of magma mixing structures occurring in three different lava flows shows that the mixing of magma is governed by chaotic dynamics associated to stretching and folding processes whose evolution in space and time produced fractal structures that propagated inside the magmatic masses over a large number of scales, from the outcrop to the microscopic scale. At any scale two main kinds of coexisting structures can be observed: (1) filament-like structures generated by intimate commingling of the magmas (active regions, AR) and (2) coherent blobs of the more basic magma that did not experience large deformation (coherent regions, CR).

Measurements of IP between the basic and acid magma and fractal dimension (D_{box}) of mixing structures reveal that linear correlations between these two parameters exist, although the three lava flows display different slopes in the linear variation of D_{box} against IP.

Simulations of magma mingling have been performed using a chaotic dynamical system in order to understand natural occurrences. Simulations reveal that a striking similarity exists between the computed structures and the structures observed in the studied lava flows. In particular, the coexistence of filament-like regions (AR) and

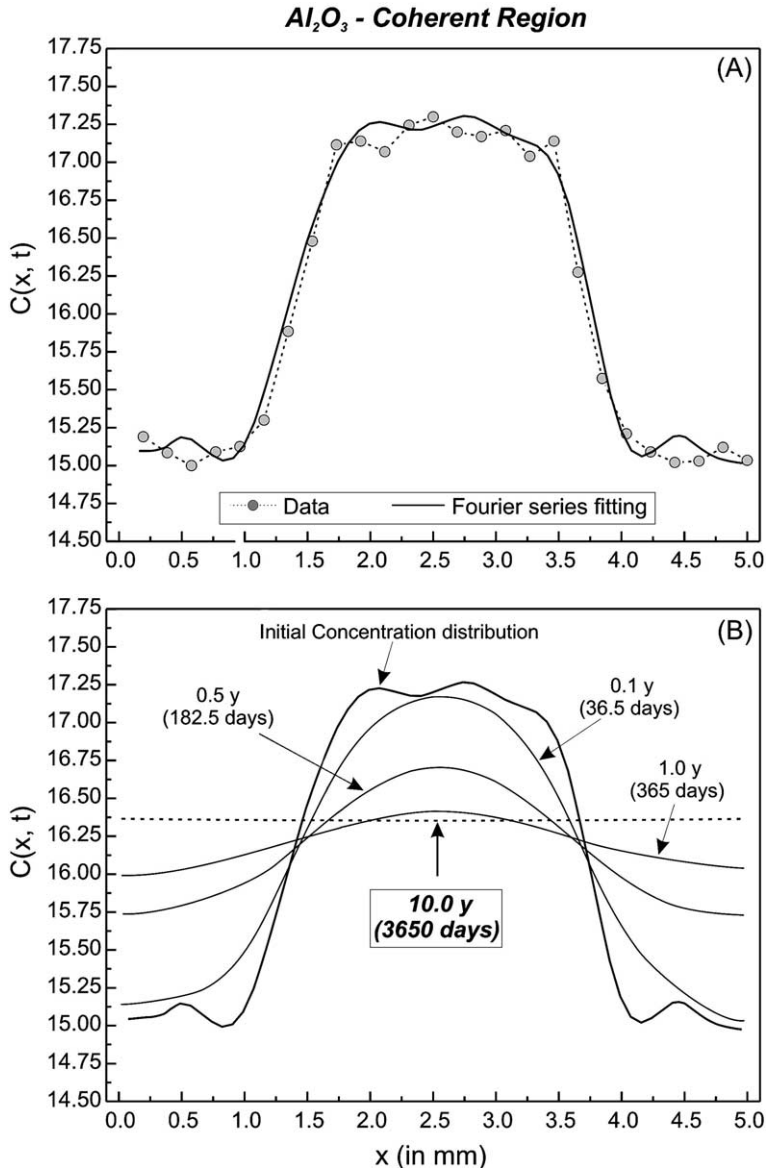

Fig. 12. Fourier series fitting (solid line) of the variation of Al_2O_3 through the coherent region of Fig. 5D (A). Variation of $C(x, t)$ against x at different times for Al_2O_3 across the coherent region (B). The dashed line in B represents the reached homogenization of the system.

coherent regions (CR) is observed in both numerical simulations and nature. IP and D_{box} have been measured for simulated magma mingling structures and linear patterns of variation between IP and D_{box} have been observed, as in natural cases. In addition, simulations evidenced that increasing slope values in the variation IP against D_{box} correspond to increasing intensities of magma mingling leading to conclude that the three different lava flows experienced different degrees of magma interaction produced by systems governed by different chaotic regimes. It is suggested that the use of IP vs. D_{box} diagrams is helpful to quantify the amount of interaction that magma

underwent in relationship to the dynamic regime that governed the magmatic system.

Physical dispersion and chemical diffusion processes are strictly related processes during mixing of magmas. Measurements on natural structures show that chemical diffusion produced different patterns of variation of chemical elements in the AR and CR. The difference in these patterns is linked to the difference in the spatial distribution of the volumes of magmas constituting AR and CR. In particular, chemical diffusion has been much more efficient in AR than in CR because the contact area between interacting magmas is much higher in AR than in CR. Simulation of chaotic mingling of magmas coupled with chemical diffusion shows that stretching and folding processes, inherent to chaotic systems, dramatically reduce the distances between the interacting magmas, owing to the production of fractal patterns within the magma body. Results show that magmatic interaction processes are able to generate in the same system volumes of magmas having extremely variable compositions in space and time. In particular, these processes can generate portions of magmas completely homogenized (AR) coexisting with portions in which magmas maintain their original compositions (CR). These results are strictly related to the local structure of flow fields induced within magma by the onset of chaotic dynamics that generate different dynamical regions (AR and CR) in which mass transfer processes act very differently in relationship with the extension of contact interfaces between interacting magmas. Such dynamical regions can propagate through a magma body from the metric to the micrometric scale, owing to the fractal nature of the process amplifying the degree of non-homogenity of magmas even at very short length scales (of the order of microns).

These results give new insights to the occurrence of magmatic enclaves found dispersed inside host rocks. Magmatic enclaves are interpreted as coherent regions of B magma that, because of the structure of flow fields inside the mixing system, did not suffer strong interactions with the more acid host rock and so survived the mixing process. It follows that host rocks can be regarded as portions of the magmatic system in which the more efficient mixing dynamics produced different degrees of hybridization.

Acknowledgements

We are grateful to S. Blake and C. Kilburn for helpful suggestions and criticisms in reviewing the manuscript. The editorial handling of B. Marsh is gratefully acknowledged. This study was funded by Italian CNR and MURST grants.

Appendix A

Chaos theory and fractal geometry

Chaos theory and fractals are closely related branches of a larger field of study whose aim is the study of complex systems. The evolution of chaos theory can be historically traced from the pioneering work of Edward N. Lorenz (Lorenz, 1963) who first realized, with the aid of computer techniques, that apparently simple systems, such as atmospheric convection, can exhibit very complex behavior. Lorenz observed that arbitrarily close particles diverged exponentially fast after few cycles of calculation depicting completely different orbits and making practically impossible to forecast the long-term evolution of the entire system. The long-term unpredictability of the Lorenz system was called 'sensitive dependence on initial conditions' and is the basic property of chaotic systems (e.g. Turcotte, 1992; Addison, 1997).

One important property of structures generated by chaotic systems is that they exhibit the same properties at many scales of magnification. Such scale invariance is known as self-similarity and is a basic property of fractal structures. Basically, a fractal is a structure that can be subdivided in parts, each of which is, at least statistically, a reduced size copy of the whole.

Chaotic systems have been recognized in a wide variety of natural processes such as atmospheric convection (Binson, 1996), plankton distribution in oceans (e.g. Abraham and Bowen, 2002), the dynamics of earthquakes (e.g. Turcotte, 1992) and

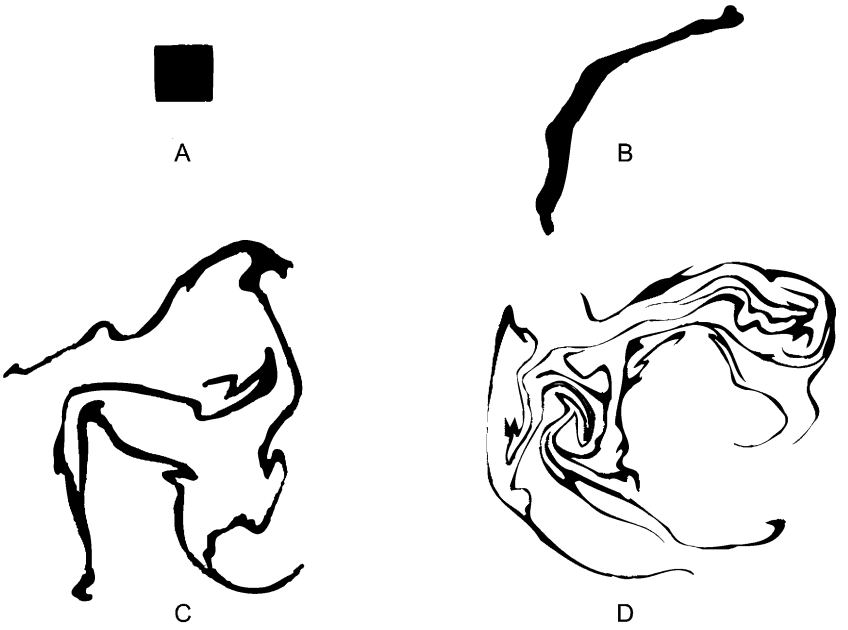

Fig. A1. Stretching and folding dynamics acting on a black colored square element of fluid (from Welander, 1955). Intensity of mixing increases from A to D.

the mixing of magmas (e.g. Poli and Perugini, 2002; Perugini et al., 2002).

Chaotic dynamics and fractals in fluid mixing

In the last years a lot of attention has been focused on the application of chaos theory and fractal geometry in the study of fluid mixing phenomena. The reason is that the basic forces promoting fluid mixing are 'stretching and folding' dynamics, and stretching and folding are also the basic dynamics leading to chaos (Ottino et al., 1988, 1993). To visualize this concept in the framework of fluid mixing processes Fig. A1 reports the outcome of a fluid dynamic experiment in which a black fluid is mixed with a white colored fluid. As the mixing time increases (from Fig. A1B to D), the original black square of fluid is progressively deformed by stretching and folding dynamics generating complex lamellar structures. Such kind of dynamical systems can be geometrically reproduced making it possible to analyze in detail their evolution. Fig. A2 shows the action of stretching and folding dynamics operating on a blob of dark fluid. As the stretching and folding dynamics proceed in time the original blob is elongated and subsequently folded over itself generating an alternation of lamellar structures that can span many orders of magnitude (Fig. A2D) producing fractal patterns. Therefore, structures produced by chaotic mixing are fractals.

Although the mixing process is chaotic, this does not imply that it is always complete. In fact, in most cases, it is very difficult to obtain a perfect mixture. The coexistence of well-mixed chaotic regions, or active regions (AR), and poorly mixed coherent regions (CR) has been, in fact, widely documented in both real and simulated fluid mixing experiments (e.g. Bresler et al., 1997; Fountain et al., 1998). Fluids inside CR can never escape and hence, they do not mix easily with the surrounding fluid whereas fluids in the AR experience strong stretching and folding processes with the surrounding fluid leading, in short times, to well mixed portions. These two kinds of regions are visible in Fig. 2A,B (main text) that show typical fluid mixing experiments in which a light and a dark colored fluid are mixed.

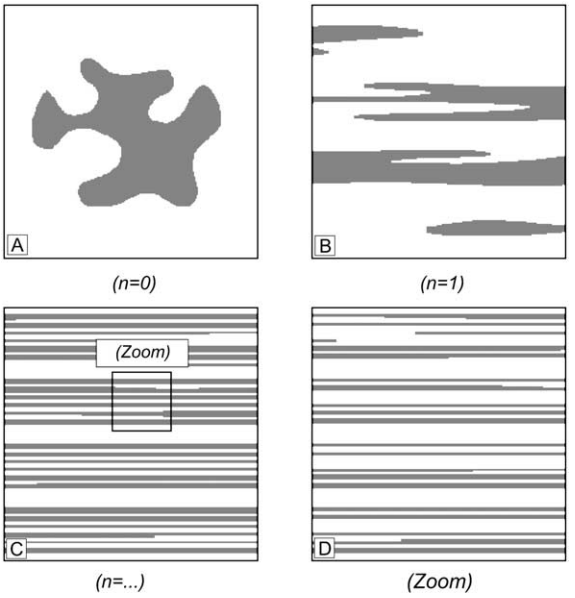

Fig. A2. Numerical simulation of stretching and folding of an original blob of dark fluid (A). During the process the portions of fluid escaping from the right side of the white square are reintroduced by the opposite side (e.g. McCauley, 1993); (D) magnification of the lamellar structures shown in (C). *n* is the time duration of the mixing process and increases from (A) to (D).

Modeling chaotic mixing

The key to understand the coexistence of these two dynamical regions within the same system lies in the study of the kinematics of fluid mixing through the use of dynamical systems. A practical way to visualize numerically these systems is to use Poincaré sections of the flow. Generally speaking a Poincaré section is a graphical representation of the flow fields of a mixing system and is useful in individuating the occurrence and the relative amount of AR and CR within the system. An example of a Poincarè section, representing a possible configuration of the cavity-flow apparatus, is reported in Fig. A3 (e.g. Liu et al., 1994b; Anderson et al., 2000). The figure shows the coexistence, within the same system, of different dynamical regions constituted by black dotted areas (representing AR) and closed orbits (representing CR).

In the study of mixing processes, major problems occur because of the sensitive dependence on initial conditions typical of chaotic systems. This characteristic limits the number of techniques that can be utilized to perform numerical simulations of mixing processes since the prediction of the long-term evolution of the systems is denied. For instance, as reported by Metcalfe et al. (1995), using conventional integration procedures in tracing individual particle trajectories during numerical experiments, differences in the velocity field greater than 0.1% can produce, after only

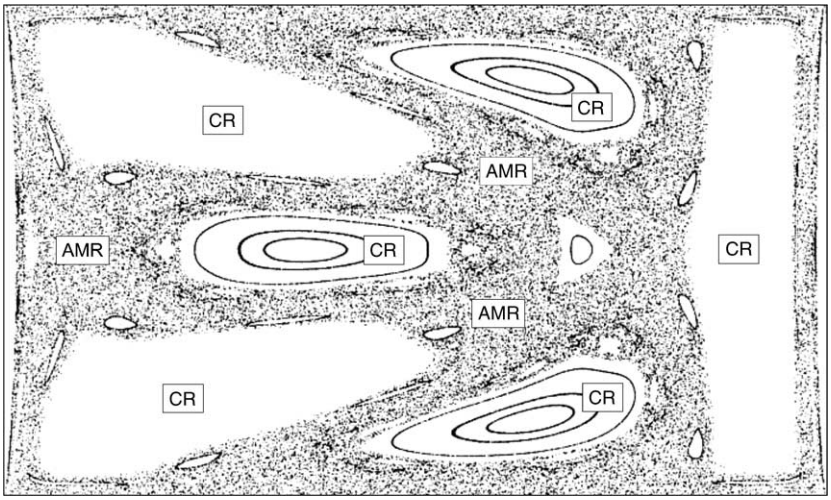

Fig. A3. Poincaré section of the dynamical system represented by the cavity-flow apparatus showing the contemporaneous occurrence of both AR and CR within the same system (from Anderson et al., 2000).

two or three circulation times, deviations of trajectories larger than the whole geometry of the system making the computation useless.

To overcome such difficulties several other techniques have been suggested and in particular the calculation of advection patterns has been recognized as one of the most suitable to simulate mixing processes (e.g. Metcalfe et al., 1995; Cerbelli et al., 2000). Underlying the concept of advection pattern is what is known as a point transformation (or 'map'), a mathematical operation that enables to identify a particle of fluid and to specify its position at some time in the future. With this technique each fluid particle is 'mapped' to a new position by the application of the transformation (or 'map') with extremely good precision avoiding the above mentioned problems. Thus, a transformation, or 'map', is a set of equations that governs the advection pattern of a mixing system.

In Fig. A4A,B are shown the patterns resulting from the simulation of mixing of real fluids in the cavity-flow apparatus, whereas Fig. A4C,D reports the patterns of the same system simulated numerically by calculating the advection patterns. The comparison between real and numerically simulated structures shows a striking similarity evidencing the reliability of the mapping approach to simulate the behavior of real fluids. It is notable that such a numerical approach is particularly useful when fluids have similar viscosities. In these conditions one fluid acts as a passive tracer because it does not influence directly the mixing process but it is advected passively within the host fluid by the action of the mixing dynamics.

The 'sine flow' map utilized in the paper to simulate mixing of magmas belongs to this category of dynamical systems. The advantage of using the sine flow map is that it captures all essential characteristics of a typical chaotic mixing system and, as such, it can be utilized as a kinematical template to simulate the chaotic mixing of magmas. In addition, the possibility to vary a single parameter (k) to generate different regimes of chaotic mixing makes this approach very suitable to explore different mixing kinematics with-

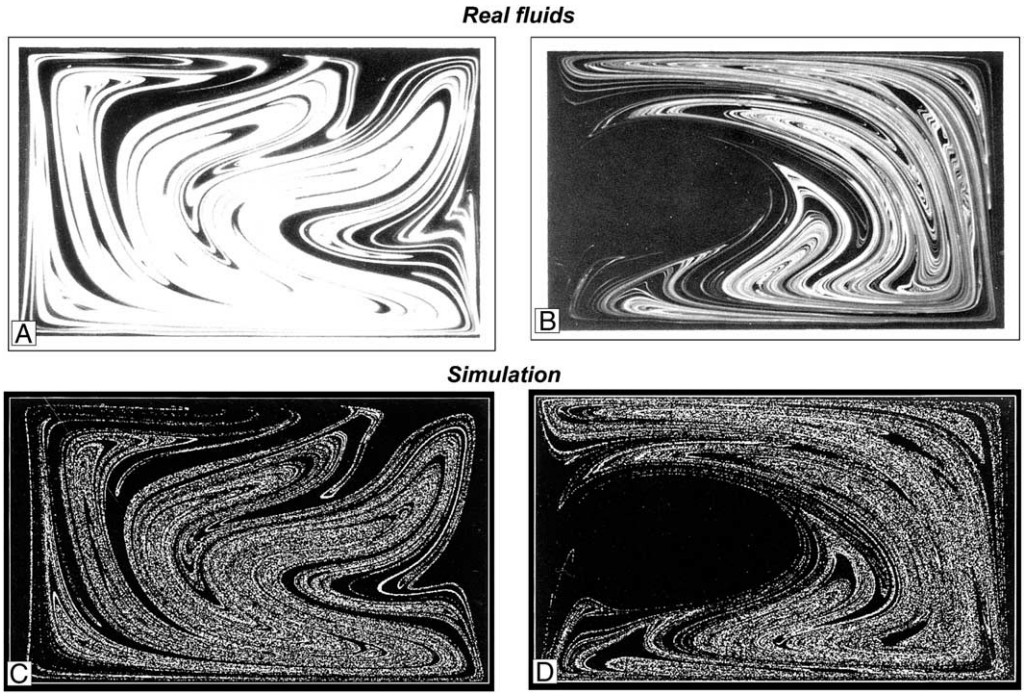

Fig. A4. (A and B) Structures generated by mixing of real fluids in the cavity-flow apparatus; (C and D) mixing structures simulated numerically by calculating the advection patterns (from Liu et al., 1994b).

out the need to keep into account the infinitely large number of parameters that influence magma mixing processes in real natural systems.

References

Abraham, E.R., Bowen, M.M., 2002. Chaotic stirring by a mesoscale surface-ocean flow. Chaos 12, 373–381.

Addison, P.S., 1997. Fractals and Chaos: an Illustrated Course. Institute of Physics Publishing, Bristol.

Albarede, F., 1995. Introduction to Geochemical Modeling. Cambridge University Press, Cambridge.

Alvarez, M.M., Muzzio, F.J., Cerbelli, S., Adrover, A., Giona, M., 1998. Self-Similar spatio-temporal structure of intermaterial boundaries in chaotic flows. Phys. Rev. Lett. 81, 3395–3412.

Anderson, P.D., Galaktionov, O.S., van de Vosse, F.N., Peters, G.W.M., Meijer, H.E.H., 2000. Mixing of non-Newtonian fluids in time-periodic cavity flows. J. Non-Newton. Fluid Mech. 93, 265–286.

Aref, H., El Naschie, M.S., 1995. Chaos Applied to Fluid Mixing. Pergamon Press, Reprinted from Chaos, Solutions and Fractals 4(6), Exeter.

Bacon, C.R., 1986. Magmatic inclusions in silicic and intermediate volcanic rocks. J. Geophys. Res. 91, 6091–6112.

Baker, D., 1990. Chemical interdiffusion of dacite and rhyolite: anhydrous measurements at 1 atm and 10 kbar, application of transition state theory, and diffusion in zoned magma chambers. Contrib. Mineral. Petrol. 104, 407–423.

Baker, D., 1991. Interdiffusion of hydrous dacitic and rhyolitic melts and the efficacy of rhyolite contamination of dacitic enclaves. Contrib. Mineral. Petrol. 106, 462–473.

Bateman, R., 1995. The interplay between crystallization, replenishment and hybridization in large felsic magma chambers. Earth-Sci. Rev. 39, 91–106.

Binson, J., 1996. Chaotic advection by Rossby-Haurwitz waves. Fluid Dyn. Res. 18, 1–16.

Blake, S., Campbell, I.H., 1986. The dynamics of magma mixing during flow in volcanic conduits. Contrib. Mineral. Petrol. 94, 72–81.

Blake, S., Fink, J.H., 2000. On the deformation and freezing of enclaves during magma mixing. J. Volcanol. Geotherm. Res. 95, 1–8.

Bresler, L., Shinbrot, T., Metcalfe, G., Ottino, J.M., 1997. Isolated mixing regions: origin, robustness and control. Chem. Eng. Sci. 52, 1623–1636.

Campbell, I.H., Turner, J.S., 1986. The influence of viscosity on fountains in magma chambers. J. Petrol. 27, 1–30.

Cardoso, S.S., Woods, A.W., 1999. On convection in a volatile-saturated magma. Earth Planet. Sci. Lett. 168, 301–310.

Cerbelli, S., Zalc, J.M., Muzzio, F.J., 2000. The evolution of material lines curvature in deterministic chaotic flows. Chem. Eng. Sci. 55, 363–371.

Chekhmir, A.S., Epel'baum, M.B., 1991. Diffusion in magmatic melts: new study. In: Perchuk, L.L., Kushiro, I. (Eds.), Physical Chemistry of Magmas. Springer, New York.

Clifford, M.J., Cox, S.M., Robert, E.P.L., 1998. Lamellar modelling of reaction, diffusion and mixing in a two-dimensional flow. Chem. Eng. J. 71, 49–56.

Clifford, M.J., Cox, S.M., Robert, E.P.L., 1999. Reaction and diffusion in a lamellar structure: the effect of the lamellar arrangement upon yield. Physica A 262, 294–306.

Collet, P., Eckman, J.P., 1980. Iterated maps on the interval as dynamical systems. In: Progress in Physics. Birkhauser, Basel.

Crank, J., 1975. The Mathematics of Diffusion. Clarendon, Oxford.

Cruden, A.R., Koyi, F., Schmeling, H., 1995. Diapirical basal entrainment of mafic into felsic magma. Earth Planet. Sci. Lett. 131, 321–340.

Davies, G.D., Halliday, A.N., Mahood, G.A., Hall, C.M., 1994. Isotopic constraints on the production rates, crystallization histories and residence times of pre-caldera silicic magmas, Long Valley, California. Earth Planet. Sci. Lett. 125, 17–37.

De Astis, G., La Volpe, L., Peccerillo, A., Civetta, L., 1997. Volcanological and petrological evolution of Vulcano Island (Aeolian Arc, Southern Tyrrhenian sea). J. Geophys. Res. 102, 8021–8050.

De Astis, G., Peccerillo, A., Kempton, P.D., La Volpe, L., Wu, T.W., 2000. Transition from calc-alkaline to potassium rich magmatism in subduction environments: geochemical and Sr, Nd, Pb isotopic constraints from the island of Vulcano (Aeolian Arc). Contrib. Mineral. Petrol. 139, 684–703.

De Rosa, R., Mazzuoli, R., Ventura, G., 1996. Relationships between deformation and mixing processes in lava flows: a case study from Salina (Aeolian Islands, Tyrrhenian Sea). Bull. Volcanol. 58, 286–297.

Ferrachat, S., Ricard, Y., 1998. Regular vs. chaotic mantle mixing. Earth Planet. Sci. Lett. 155, 75–86.

Flinders, J., Clemens, J.D., 1996. Non-linear dynamics, chaos, complexity and enclaves in granitoid magmas. Trans. R. Soc. Edinburgh Earth Sci. 87, 225–232.

Fountain, G.O., Khakhar, D.V., Ottino, J.M., 1998. Visualization of three-dimensional chaos. Science 281, 683–686.

Gertisser, R., Keller, J., 2000. From basalt to dacite: origin and evolution of the calc-alkaline series of Salina, Aeolian Arc, Italy. Contrib. Mineral. Petrol. 139, 607–626.

Grasset, O., Albarede, F., 1994. Hybridisation of mingling magmas with different densities. Earth Planet. Sci. Lett. 121, 327–332.

Heath, E., Turner, S.P., Macdonald, R., Hawkesworth, C.J., van Calsteren, P., 1998. Long magma residence times at an island arc volcano (Soufriere, St. Vincent) in the Lesser Antilles evidence from ^{238}U–^{230}Th isochron dating. Earth Planet. Sci. Lett. 160, 49–63.

Hydon, P.E., 1995. Resonant and chaotic advection in a curved pipe. In: Aref, H., El Naschie, M.S. (Eds.), Chaos Applied to Fluid Mixing. Pergamon Press, Reprinted from Chaos, Solutions and Fractals 4(6), Exeter, pp. 197–210.

Jain, A.K., 1989. Fundamentals of Digital Image Processing, Prentice-Hall, New Jersey.

Koyaguchi, T., Blake, S., 1989. The dynamics of magma mixing in a rising magma batch. Bull. Volcanol. 52, 132–137.

Koyaguchi, T., 1985. Magma mixing in a conduit. J. Volcanol. Geotherm. Res. 25, 265–369.

Kuo, C., Cabarcos, E.L., Scala, A., Bansil, R., 1997. Kinetics of spatially confined precipitation and periodic pattern formation. Physica A 239, 390–403.

Liebovitch, L., Toth, T., 1989. A fast algorithm to determine fractal dimension by box counting. Phys. Lett. A 141, 386–390.

Liu, M., Muzzio, F.J., Peskin, R.L., 1994a. Quantification of mixing in aperiodic chaotic flows. Chaos Solutions Fractals 4, 869–893.

Liu, M., Peskin, R.L., Muzzio, F.J., Leong, C.W., 1994b. Structure of the stretching field in chaotic cavity flows. Am. Inst. Chem. Eng. J. 40, 1273–1286.

Lorenz, E., 1963. Deterministic non-periodic flow. J. Atmos. Sci. 20, 130–141.

Mandelbrot, B.B., 1982. The Fractal Geometry of Nature. W.H. Freeman, New York.

McCauley, J.L., 1993. Chaos, Dynamics and Fractals: an Algorithmic Approach to Deterministic Chaos. Cambridge University Press, Cambridge.

Meleshko, V.V., Van Heijst, G.J.F., 1995. Interacting two-dimensional vortex structures: point vortices, contour kinematics and stirring properties. In: Aref, H., El Naschie, M.S. (Eds.), Chaos Applied to Fluid Mixing. Pergamon Press, Reprinted from Chaos, Solutions and Fractals 4(6), Exeter, pp. 233–266.

Metcalfe, G., Bina, C.R., Ottino, J.M., 1995. Kinematic considerations for mantle mixing. Geophys. Res. Lett. 22, 743–746.

Muzzio, F.J., Swanson, P.D., Ottino, J.M., 1992. Mixing distributions produced by multiplicative stretching in chaotic flows. Int. J. Bif. Chaos 2, 37–50.

Oldenburg, C.M., Spera, F.J., Yuen, D.A., Sewell, G., 1989. Dynamic mixing in magma bodies: theory, simulations and implications. J. Geophys. Res. 94, 9215–9236.

Ott, E., Antonsen, T.M., Jr., 1989. Chaotic fluid convection and the fractal nature of passive scalar gradients. Phys. Rev. Lett. 61, 2839–2842.

Ottino, J.M., 1989. The Kinematics of Mixing: Stretching, Chaos and Transport. Cambridge University Press, Cambridge.

Ottino, J.M., Leong, C.W., Rising, H., Swanson, P.D., 1988. Morphological structures produced by mixing in chaotic flows. Nature 333, 419–425.

Ottino, J.M., Muzzio, F.J., Tjahjadi, M., Franjione, J.G., Jana, S.C., Kusch, H.A., 1993. Chaos, symmetry, and self-similarity: exploiting order and disorder in mixing processes. Science 257, 754–760.

Pe-Piper, G., Piper, D.J.W., 1992. Geochemical variation with time in the Cenozoic high-K volcanic rocks of the island of Lesbos, Greece: significance for shoshonite petrogenesis. J. Volcanol. Geotherm. Res. 53, 371–387.

Pe-Piper, G., 1984. Zoned pyroxenes from shoshonite lavas of Lesbos, Greece: inferences concerning shoshonite petrogenesis. J. Petrol. 25, 453–472.

Perugini, D., Busà, T., Poli, G., Nazzareni, S., 2003. The role of chaotic dynamics and flow fields in the development of disequilibrium textures in volcanic rocks. J. Petrol. 44, 733–756.

Perugini, D., Poli, G., Gatta, G., 2002. Analysis and simulation of magma mixing processes in 3D. Lithos 65, 313–330.

Perugini, D., Poli, G., Prosperini, N., 1999. Magma mixing and dynamical systems: a new approach for the study of magmatic interaction phenomena. In: Lippard, S.J., Naess, A., Sinding-Larsen, R. (Eds.), Proceedings of the fourth annual conference of the International Association for Mathematical Geology. Trondheim, pp. 239–244.

Perugini, D., Poli, G., 2000. Chaotic dynamics and fractals in magmatic interaction processes: a different approach to the interpretation of mafic microgranular enclaves. Earth Planet. Sci. Lett. 175, 93–103.

Pierrehumbert, R.T., 1995. Tracer microstructures in the large-eddy dominated regime. In: Aref, H., El Naschie, M.S. (Eds.), Chaos Applied to Fluid Mixing. Pergamon Press, reprinted from Chaos, Solutions and Fractals 4(6) Exeter.

Pietruszka, A.J., Garcia, M.O., 1999. The size and shape of Kilauea Volcano's summit magma storage reservoir: a geochemical probe. Earth Planet. Sci. Lett. 167, 311–320.

Poli, G., Perugini, D., 2002. Strange attractors in magmas: evidence from lava flows. Lithos 65, 287–297.

Poli, G., Tommasini, S., 1991. Origin and significance of microgranular inclusions in calc-alkaline granitoids: a proposed working model. J. Petrol. 32, 657–666.

Poli, G., Tommasini, S., Halliday, A.N., 1996. Trace elements and isotopic exchange during acid–basic magma interaction processes. Trans. R. Soc. Edinburgh Earth Sci. 87, 225–232.

Schreiber, U., Anders, D., Koppen, J., 1999. Mixing and chemical interdiffusion of trachytic and latitic magma in a subvolcanic complex of the Tertiary Westerwald (Germany). Lithos 46, 695–714.

Sepulveda, M.A., Badii, R., Pollak, E., 1989. Spectral analysis of conservative dynamical systems. Phys. Rev. Lett. 63, 1226–1229.

Shaw, H.R., 1972. Viscosities of magmatic silicate liquids: An empirical method of prediction. Am. J. Sci. 272, 870–893.

Snyder, D., Tait, S.R., 1996. Magma mixing by convective entrainment. Nature 379, 529–531.

Sparks, S.R.J., Marshall, L.A., 1986. Thermal and mechanical constraints on mixing between mafic and silicic magmas. J. Volcanol. Geotherm. Res. 29, 99–124.

Sreenivasan, K.R., Prasad, R.R., Mendeveau, C., Ramshankar, R., 1989. The fractal geometry of interfaces and the multifractal distribution of dissipation in fully turbulent flows. In: Scholtz, C.H., Mandelbrot, B.B. (Eds.), Fractals in Geophysics. Birkhauser Verlag, Basel, pp. 43–60.

Thomas, N., Tait, S.R., 1997. The dimensions of magmatic inclusions as a constraint on the physical mechanism of mixing. J. Volcanol. Geotherm. Res. 75, 167–178.

Turcotte, D.L., 1992. Fractals and Chaos in Geology and Geophysics. Cambridge University Press, Cambridge.

Volpe, T.A., Hammond, P.E., 1991. ^{238}U–^{230}Th–^{226}Ra disequilibria in young Mount St. Helens rocks: time constraints for magma formation and crystallization. Earth Planet. Sci. Lett. 107, 475–486.

Vorobieff, P., Righley, P.M., Benjamin, R.F., 1999. Shock-driven gas curtain: fractal dimension evolution in transition to turbulence. Physica D 33, 469–476.

Weinberg, R.F., Leitch, A.M., 1998. Mingling in mafic magma chambers replenished by light felsic inputs: fluid dynamical experiments. Earth Planet. Sci. Lett. 157, 41–56.

Welander, P., 1955. Studies on the general development of motion in a twodimensional, ideal fluid. Tellus 7, 141–156.

Williams, Q., Tobisch, T., 1994. Microgranitic enclave shapes and magmatic strain histories: constraints from drop deformation theory. J. Geophys. Res. 99, 24359–24368.

Woods, A.W., Pyle, D.M., 1997. The control of chamber geometry on triggering on volcanic eruptions. Earth Planet. Sci. Lett. 151, 155–166.